Journal of Optics

PAPER

Soliton refraction and Goos–Hänchen shifts at diffusion step nonlocal interfaces

IOP Publishing Journal of Optics
J. Opt. 22 (2020) 015502 (9pp) https://doi.org/10.1088/2040-8986/ab5823

Soliton refraction and Goos–Hänchen shifts at diffusion step nonlocal interfaces

J Sánchez-Curto and P Chamorro-Posada

Departamento de Teoría de la Señal y Comunicaciones e Ingeniería Telemática, Universidad de Valladolid, ETSI Telecomunicación, Paseo Belén 15, 47011 Valladolid, Spain

E-mail: julsan@tel.uva.es

Received 12 April 2019, revised 20 October 2019
Accepted for publication 15 November 2019
Published 16 December 2019

Abstract

Diffusive Kerr-type interfaces separating media that differ only in their diffusion strength are studied within the Helmholtz framework. We obtain an analytical expression for a soliton effective nonlinear refractive index that takes into account diffusion. A discontinuity in this coefficient makes a soliton undergo external refraction after entering a second medium with a higher diffusion strength. Our theory also predicts total internal reflection and giant Goos–Hänchen shifts when the diffusion is higher in the first medium. Numerical simulations are used to test the validity of the model, showing excellent agreement with theoretical predictions.

Keywords: nonlinear interfaces, Snell's law, diffusive Kerr-type media

1. Introduction

Interfaces constitute one of the most appealing subjects within the field of nonlinear optics. Initially studied for boundaries separating local media, they have been revisited in the case of nonlocal media where nonlocality has revealed substantial changes in relation to their local counterparts. Such is the case of diffusive Kerr-type interfaces [1] where the diffusion of carriers was demonstrated to enhance the formation of nonlinear surface waves [2, 3] or to modify the local response of the interface [4] within the particle-like approach [5]. More recently, the interface between thermal media [6, 7] has been shown to accommodate surface waves [8] or surface dipoles and vortices [9]. Planar boundaries that confine a strongly thermal medium have been also proposed for controlling soliton trajectories within the sample [10]. As regards nematicons [11], the ease of implementation of nonlinear interfaces within a nematic crystal cell [12] has permitted the experimental study of tunable nematicon reflection or refraction [12], non-specular reflection [13], giant Goos–Hänchen shifts [14] or even anomalous (negative) refraction [15]. Based on these studies, nematic crystal valves have been proposed as candidates for optical switching devices [16–18].

While analytic models have changed in order to describe the variety of nonlocal responses, the paraxial approximation assumed in the propagation equations has remained in most works. This issue was already considered in the case of highly nonlocal media [19, 20] and solutions were later reported for two nonparaxial contexts, i.e. narrow beams in relation of its wavelength, which demand a vector treatment of the problem [21, 22], and scenarios of on-axis nonparaxiality where the beam undergoes rapid changes in its envelope [23]. We are, however, interested in the nonparaxiality of angular character that arises when the soliton envelope changes on propagating off-axis. This type of nonparaxiality is intrinsic to the optics of interfaces and it must be included in the analysis.

The literature on interfaces separating nonlocal media also reveals that the numerical work plays an essential role in order to describe soliton behavior at interfaces [10, 12]. The complexity of the propagation models for nonlocal media leads to the absence of analytic results explicitly connecting the strength of the nonlocality with soliton refraction properties at the interface.

This work tries to overcome these two issues for the case of interfaces separating diffusive Kerr-type media that only differ on the strength of carrier diffusion, i.e. diffusion step nonlocal interfaces. First, our approach is developed within the Helmholtz theory, thus removing the angular restrictions associated to the paraxial approximation. Second, we provide analytic results which capture the relationship between angles of refraction and the nonlocal properties of the adjoining media. Our analysis reveals that diffusion step nonlocal interfaces accommodate, in principle, an unexpected soliton refraction, in the sense that external (internal) refraction is obtained when the diffusion strength is higher (lower) in the second medium.

The paper presents, in section 2, a brief review of the existing Helmholtz theory, which is essential to contextualize this work. The study of nonlocal interfaces is developed in section 3 where the connection between angles and nonlocality, the existence of critical angles or the formation of giant Goos–Hänchen shifts are analytically predicted and numerically tested. Conclusions are summarized in section 5.

2. The Helmholtz framework

The Helmholtz theory [24–26] has overcome the limitations of paraxial analyses [27] when it comes to addressing the evolution of broad beams that propagate at arbitrary angles. This framework is based on the nonlinear Helmholtz (NLH) [28] equation, which is fully equivalent to the corresponding 2D Helmholtz equation and represents a generalization of the nonlinear Schrödinger [29, 30] equation. Initially presented for Kerr-focusing media, the theory has been successfully developed for other types of nonlinear media, such as Kerr defocusing [31], cubic-quintic [32, 33], power-law [34] or saturable [35] materials. In all these works, the properties of Helmholtz solitons have been properly addressed and essential corrections to their paraxial counterparts have been highlighted. More recently, this Helmholtz treatment has been applied to the study of nonlocal media where nonlocality arises from the diffusion of carriers [36].

The type of nonparaxiality addressed in the NLH is of angular type, which turns it into an excellent tool to deal with problems of an inherent angular content. Such is the case of soliton collisions [37] and, basically, interfaces, which have deserved our attention during recent years. The preservation of the complete angular content of the problem has been summarized in a compact Snell's law [38], which addresses the reflection and refraction of not only bright [39–41], but black [42] and gray [43] solitons. The analysis has been recently extended to the case of nonlocal interfaces where novel properties, such as its dual switching behavior, have been found whenever local and nonlocal mismatches are properly combined [44].

The equation that rules the Helmholtz analysis of such interfaces was presented in [44] and reads as follows:

$$\kappa\frac{\partial^2 u}{\partial\zeta^2}+i\frac{\partial u}{\partial\zeta}+\frac{1}{2}\frac{\partial^2 u}{\partial\xi^2}+u(|u|^2+d_{01}^2\phi_{nl})=H(\xi)u\left[\frac{\Delta}{4\kappa}+(1-\alpha)|u|^2+(d_{01}^2-\alpha d_{02}^2)\phi_{nl}\right]. \quad (1)$$

u is the complex envelope of a propagating TE electromagnetic field [45], $\xi=2^{1/2}x/w_0$ and $\zeta=z/L_D$ are the normalized transverse and longitudinal coordinates, respectively, being w_0 the beam width of a reference Gaussian beam and $L_D=kw_0^2/2$ the diffraction length. $\kappa=1/k^2w_0^2$ is the nonparaxiality parameter that accounts for the soliton width in relation to the optical wavelength [25, 26], while $\Delta=1-n_{02}^2/n_{01}^2$ and $\alpha=\alpha_2/\alpha_1$ are the local linear and nonlinear mismatching parameters, respectively [38]. $H(\xi)$ is the Heaviside function that addresses the first ($H(\xi)=0$ if $\xi<0$) or the second ($H(\xi)=1$ if $\xi\geqslant 0$) medium. As regards the nonlocal contribution, d_{01} and d_{02} are the normalized diffusion coefficients in each medium [36, 44], while ϕ_{nl} is the nonlocal contribution to the refractive index [36]:

$$\phi_{nl}=\frac{\partial^2|u|^2}{\partial\xi^2}+2\kappa\frac{\partial^2|u|^2}{\partial\zeta^2}. \quad (2)$$

Table 1. Particularizations of (1) to address different Helmholtz scenarios.

	$\Delta=0,\ \alpha=1$	$\Delta\neq 0,\ \alpha\neq 1$
$d_{0i}=0$	local media [25, 26, 28]	local interfaces [38, 42, 43]
$d_{01}=d_{02}$	nonlocal media [36]	—
$d_{01}\neq d_{02}$	*diffusion step nonlocal interfaces*	nonlocal interfaces [44]

Table 1 provides an overview of previous Helmholtz works on Kerr-like local and nonlocal interfaces.

Table 1 reveals that the study of interfaces has so far been incomplete, lacking a previous analysis of *diffusion step nonlocal interfaces*. Previous paraxial studies on diffusive Kerr-type interfaces have always considered a linear mismatch ($\Delta\neq 0$) [2, 4], which essentially veils the effect of nonlocality on soliton behavior at the interface.

The analysis we perform in this work is based on the formalism presented in [44], which, in turn, builds upon previous results of [36]. In [44], however, this general formalism is used exclusively for studying the dual switching behavior that arises under a specific combination of changes in the local and nonlocal contributions to the refractive index across the interface. In this paper, in contrast, we address the effects observed under a perfect match of the terms contributing to the nonlinear refractive index that have a local character and, therefore, an interface mismatch affected only by diffusion. In this type of diffusion step nonlocal interfaces we find new and relevant effects. We determine how the change of the diffusion parameter across the interface alone rules the refraction properties of solitons passing over the interface. In particular, we discover internal refraction behavior when the first medium has a larger diffusion strength. This, in principle, unexpected effect is analyzed in detail and explained using the theory of [44]. As is normally the case in nonlinear interfaces with internal refraction, our analysis confirms the observation of the giant Goos–Hänchen shift. We want to stress that the existence of this effect due to a discontinuity on the nonlocality alone is far from trivial. Also, as opposed to other nonlinear scenarios [38, 43], diffusion step nonlocal interfaces lack a full transparency condition.

3. Diffusion step nonlocal interfaces

The analysis of diffusion step nonlocal interfaces is based on approximating the response of the diffusive Kerr medium by a

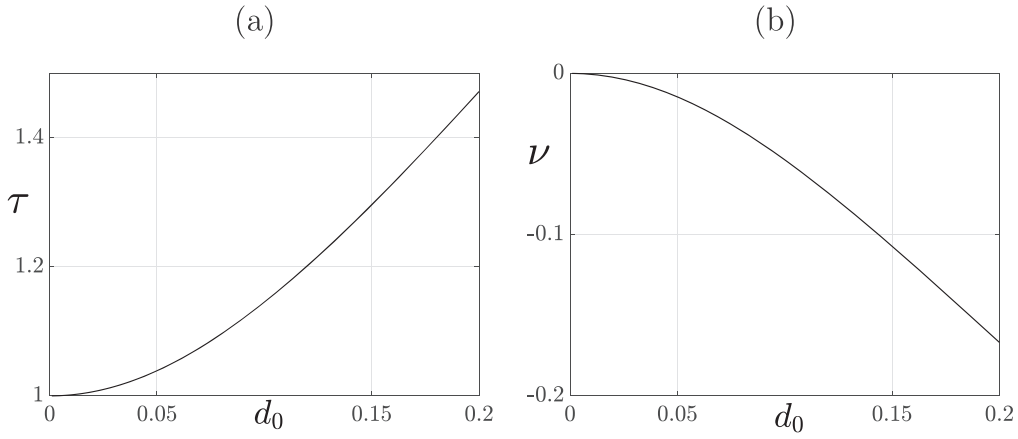

Figure 1. Evolution of the cubic (a) and quintic (b) parameters with the diffusion strength. In both cases, the Helmholtz soliton amplitude is $\eta_0 = 2$.

cubic-quintic model [44]:

$$\phi = |u|^2 + d_0^2\phi_{nl} \approx \tau|u|^2 + \nu|u|^4, \tag{3}$$

where τ and ν are the effective cubic and quintic parameters, respectively. They are plotted, for $\eta_0 = 2$, in figure 1 as a function of d_0. ν is associated to the peak reduction in the nonlinear response of the soliton ϕ_{nl}. τ and ν together are responsible for the spatial broadening of the soliton nonlinear response in the diffusive Kerr medium. In the local case ($d_0 = 0$), one has the Kerr response without any sort of corrections, i.e. $\tau = 1$ and $\nu = 0$.

Imposing the phase continuity across the interface to the cubic-quintic soliton solutions that result from the former approximation, we conclude that Helmholtz solitons at diffusion step nonlocal interfaces are ruled by:

$$\gamma \cos\theta_i = \cos\theta_t, \tag{4}$$

where θ_i and θ_t are the angles of incidence and refraction defined in relation to the interface, respectively, and γ is a nonlinear correction term that reads as follows:

$$\gamma = \left[\frac{1 + 2\kappa\eta_0^2\left(1 + \frac{2}{3}\eta_0^2\sigma_1\right)}{1 + 2\kappa\eta_0^2\left(\tau_2/\tau_1 + \frac{2}{3}\eta_0^2\sigma_2\right)}\right]^{1/2}, \tag{5}$$

where subscripts $i = 1, 2$ refer to the first and second medium, respectively. $\sigma_i = \nu_i/\tau_1^2$ displays a slower variation as the diffusion strength grows, compared to ν_i since $\tau_1 \geqslant 1$ and τ_1 also increases with the diffusion coefficient. The Helmholtz term $2\kappa\eta_0^2$ in (5) reveals that the angular deflection at the interface is intrinsically nonparaxial. In the paraxial limit, when one works with very broad beams in relation to the wavelength ($\kappa \to 0$) of low intensity ($2\kappa\eta_0^2 \to 0$), one has $\gamma \to 1$, and no changes in the soliton angle of propagation could be found at the interface. This can explain the absence of paraxial works on this type of interface.

Soliton evolution at diffusion step nonlocal interfaces is basically ruled by the sign and magnitude of $d_{01} - d_{02}$. The soliton can undergo external (internal) refraction if $d_{01} < d_{02}$ ($d_{01} > d_{02}$) and the higher the difference between the nonlocal responses of the two media, the larger the deflection on the soliton direction of propagation. This can be observed in figure 2(a), which displays the contours of γ as a function of the strength of the diffusion in each medium. The straight line represents the curve $\gamma = 1$ and establishes the transition from internal to external refraction. Since this curve is obtained only if $d_{01} = d_{02}$, we conclude that, in contrast to other interface configurations [38], an intensity driven total transparency condition cannot be set in a step nonlocal interface.

By making $\gamma = n_1/n_2$, one obtains the definition of a soliton effective nonlinear refractive index in each medium that only depends on the diffusion strength. Values for n_1 and n_2 can be obtained from figures 1(a) and (b), so that for a nonlocal medium with $d_{01} = 0.2$, for instance, one has $\tau_1 = 1.471\,8$ and $\sigma_1 = -0.077$, thus giving $n_1 = 1.008$. The corresponding counterparts for a local ($d_{02} = 0$) medium are $\tau_2 = 1$ and $\sigma_2 = 0$, being $n_2 = 1.006$. We have assumed in the calculations that the Helmholtz term is $2\kappa\eta_0^2 = 0.02$.

The validity of our analytical findings is tested with the full numerical integration of the evolution equations given by (1) and (2) when $\Delta = 0$ and $\alpha = 1$. This is carried out using the nonlinear beam propagation method (NBPM) [46], which is particularly well suited for addressing the problem of solitons propagating at arbitrary angles impinging on interfaces whose relative differences between their refractive indexes are small. Exact Helmholtz soliton solutions in the first medium at $\zeta_0 = 0$ and $\zeta_1 = \Delta\zeta$ are used as initial conditions in the algorithm, while the new propagation conditions found at the interfaces act as a small perturbation. The reliability of the NBPM has been tested with the numerical integration of the corresponding 2D time-domain Maxwell equations based on the transmission line method [45] and a detailed assessment of its accuracy and applicability conditions has been presented in [47].

A set of simulations has been performed for different values of κ, d_{0i} and η_0. Figure 2(b) displays with points θ_t as a function of θ_i for the case of $\kappa = 2.5 \times 10^{-3}$ and $\eta_0 = 2$ when different values of d_{0i} are used. In order to focus on the effect of nonlocality on the angle of refraction, we have always imposed $d_{0i} = 0$ in one of the two media, thus working with nonlocal-local or local-nonlocal interfaces. Only low angles of incidence and refraction are displayed

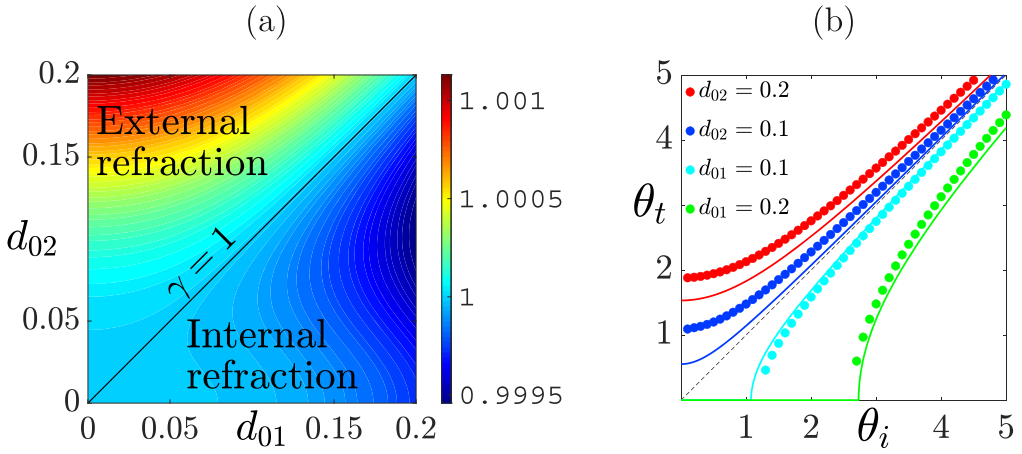

Figure 2. Contours of γ as a function of d_{01} and d_{02} (a). θ_t as a function of θ_i at a diffusion step nonlocal interface for different values of d_{01} and d_{02} (b).

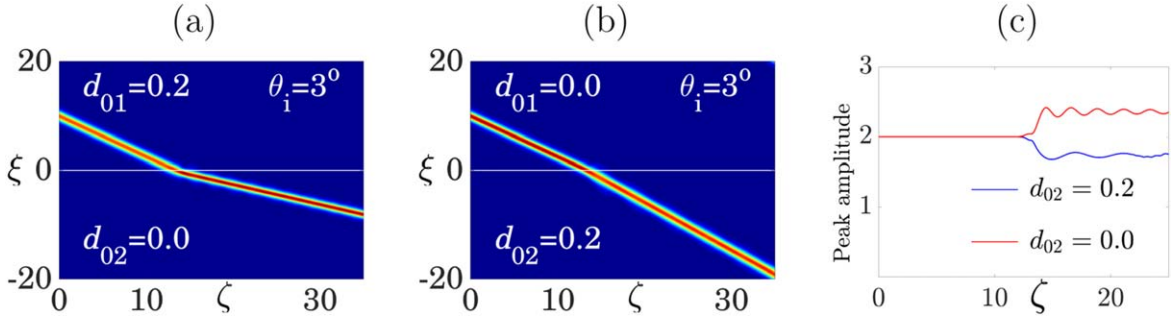

Figure 3. Soliton undergoing internal (a) or external (b) refraction when $d_{01} > d_{02}$ or $d_{01} < d_{02}$, respectively, when $\theta_i = 3°$. Evolution of the soliton peak amplitude for the case of internal (red) and external (blue) refraction.

because we restrict the analysis to the small d_{0i} weakly nonlocal regime where the effective nonlinear indexes are also small. Solid lines correspond to the prediction displayed in (4) and (5) for the same values used in simulations.

In [44], figure 4(d) shows a soliton undergoing internal refraction at an interface with $\Delta = -0.000\,1$, $\alpha = 0.87$, $d_{01} = 0$ and $d_{02} = 0.2$. The soliton amplitude is 2 and the angle of incidence is 1 degree. The red line of figure 2(b) shows that this soliton undergoes just the opposite behavior (external refraction) at a diffusion step nonlocal interface when the same nonlocal parameters are used. This divergence in the interface response lies on the different working regimes we assume in [44] and this work. In [44], local and nonlocal contributions are of the same order of magnitude, so that the role of the diffusion is limited to counteract the local mismatch by adding a quadratic dependence on soliton intensity. This contribution is essential to induce the dual switching behavior of the interface reported in [44]. In this work, however, by assuming $\Delta = 0$ and $\alpha = 1$ we ensure that the working regime is only ruled by the nonlocal contribution, so that we are able to isolate the impact of diffusion on the interface and, in turn, reveal the effects reported in this work.

The contour plots of figures 3(a) and (b) correspond to the green and red series of figure 2(b), respectively, when $\theta_i = 3°$. Figure 3(a) shows that the soliton undergoes internal refraction when the diffusion is higher in the first medium. The explanation for this, in principle, contradictory result lies in the spatial broadening of the soliton refractive index response ϕ_{nl} [44] in a diffusive Kerr medium, which represents a barrier to soliton propagation whenever $d_{01} > d_{02}$. The same reason explains the opposite behavior shown in figure 3(b), where the soliton undergoes external refraction after entering a second medium with a higher diffusion strength. This effect has not been addressed in our previous works [38, 43] where the magnitude of the local linear and nonlinear mismatch would mask a hypothetical nonlocal response like this. Figure 3(c) captures the peak amplitude of the two solitons displayed in figures 3(a) and (b). As the red (blue) line shows, soliton amplitude increases (decreases) when the diffusion strength of the second medium is lower (higher). Taking into account the preservation of the power flow across the interface, one can thus infer the subsequent changes in soliton width.

3.1. Critical angle

The absence of data points in figure 2(b) for small angles of incidence when $d_{01} > d_{02}$ suggests that critical angles can be found when the diffusion is higher in the first medium. An example is shown in the contour plot of figure 4(a), which illustrates soliton behavior for the same set of parameters used in figure 3(a) when the angle of incidence is not $\theta_i = 3°$, but $\theta_i = 1.7°$.

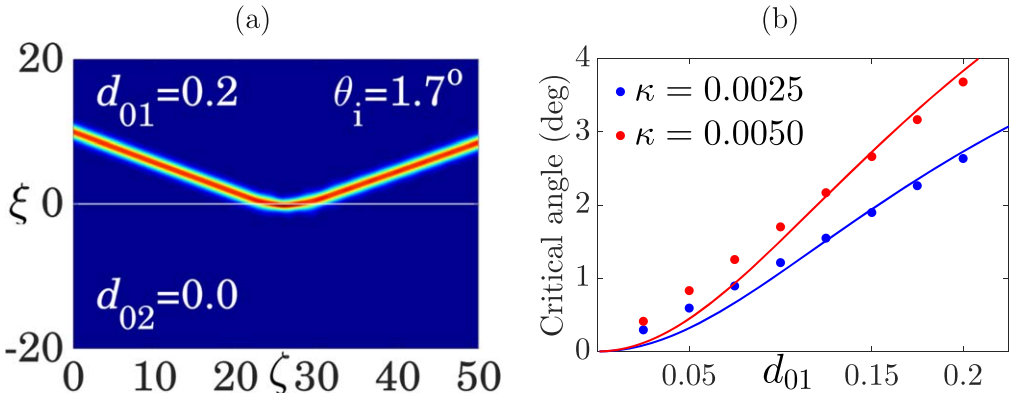

Figure 4. Soliton undergoing internal reflection (a). Critical angle as a function of d_{01} for two different values of κ (b).

Making $\theta_t = 0$ in (4), we obtain an expression for the critical angle θ_c:

$$\tan^2\theta_c = \frac{2\kappa\eta_0^2\left[\left(1-\tau_2/\tau_1\right)+\frac{2}{3}\eta_0^2(\sigma_1-\sigma_2)\right]}{1+2\kappa\eta_0^2\left(\tau_2/\tau_1+\frac{2}{3}\eta_0^2\sigma_2\right)}, \tag{6}$$

which is a particularization of the result of [44] for $\Delta = 0$ and $\alpha = 1$. Equation (6) can be rewritten for a nonlocal-local interface ($d_{02} = 0$) as:

$$\tan^2\theta_c = \frac{2\kappa\eta_0^2\left[(1-\tau_1^{-1})+\frac{2}{3}\eta_0^2\sigma_1\right]}{1+2\kappa\eta_0^2\tau_1^{-1}}. \tag{7}$$

Equation (7) is plotted in figure 4(b) with solid lines as a function of d_{01} when two different values of κ are used. The larger the difference between adjoining diffusion coefficients, the higher the value of the critical angle. Points in figure 4(b) correspond to the numerical results extracted from the integration of (1) and (2).

Figure 4(b) also shows that the interface impact on soliton evolution is enhanced as the nonparaxiality parameter κ increases. Although soliton propagation in diffusive Kerr-type media has been demonstrated to depend on its width [48], such dependency has not been addressed before in the case of interfaces where the beam width is missing in the analysis [4]. Our Helmholtz treatment can capture this effect through κ.

3.2. Giant Goos–Hänchen shifts

Nonlinear interfaces can accommodate giant Goos–Hänchen shifts (GHSs) in a great variety of interface configurations separating not only local [5, 40, 49–53], but highly [14] and weakly [54] nonlocal media. Since GHSs arise when the angle of incidence approaches the critical angle, we show in this work that GHSs can appear when the diffusion is higher in the first medium.

Equation (7) provides the combination of soliton intensity (through $2\kappa\eta_0^2$) and nonlocal response (through σ_1 and τ_1) where GHSs are prone to appear. One just needs to work in the vicinity of θ_c, so that this phenomenon can be obtained. Figure 5(a) shows a soliton undergoing a giant GHS ζ_0 for a nonlocal-local interface when the soliton amplitude is $\eta_0 = 2$ and propagates at an angle of $\theta_i = 2.6353°$. This value of θ_i has been chosen just below the predicted critical angle, which is $\theta_c = 2.73°$.

Figure 5(b) shows in blue the numerical calculation of the GHS based on the integration of (1) and (2) for the same interface, while the red vertical line represents the value of θ_c given by (7). The giant GHS grows exponentially as θ_i approaches θ_c, thus showing the accuracy of our analytical results to predict this phenomenon at diffusion step nonlocal interfaces.

The analysis presented in this work applies only to the 2D case. Even though the evolution equations (1) and (2) can be directly extended to 3D, the analytical results, like Snell's law, have been derived from the 2D exact soliton solutions. These analytical results cannot be continued to the 3D case, since no corresponding exact solutions have been found in a 3D model. However, the extension of the NBPM to two transverse dimensions [46] can provide us with the angular content that is missing in the paraxial study of interfaces separating not only diffusive Kerr media, but materials exhibiting a cubic-quintic response [55–57].

A realistic configuration for engineering a nonlocal step interface could rely on the ability of effectively tailoring the linear and nonlinear refractive indexes of different types of glasses via doping, for example [58]. Therefore, a possible route to implement such an interface could be to use a glass that is linear and nonlinear index matched ($\Delta = 0$ and $\alpha = 1$) to a second medium with a thermal nonlocal nonlinearity. This second medium could be a lead glass [59], polymer [60], or solution [61], and the first glass could have either a nonlocal or local response, the latter case providing a local-nonlocal step interface.

4. Sensitivity to interface parameters

Throughout this work, we have presented the effects found at diffusion step nonlocal interfaces. In this section, however, we consider $\Delta \neq 0$ and $\alpha \neq 1$ in order to explore the

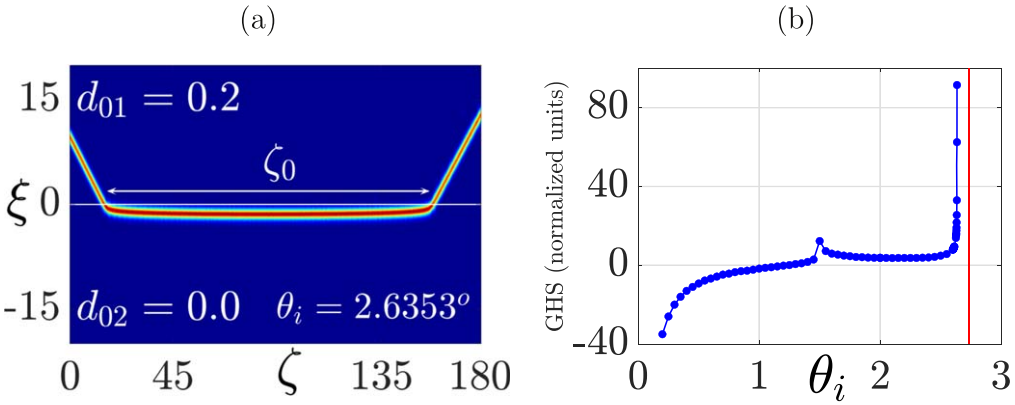

Figure 5. Soliton undergoing a giant GHS (a). Evolution of the GHS as a function of θ_i (b).

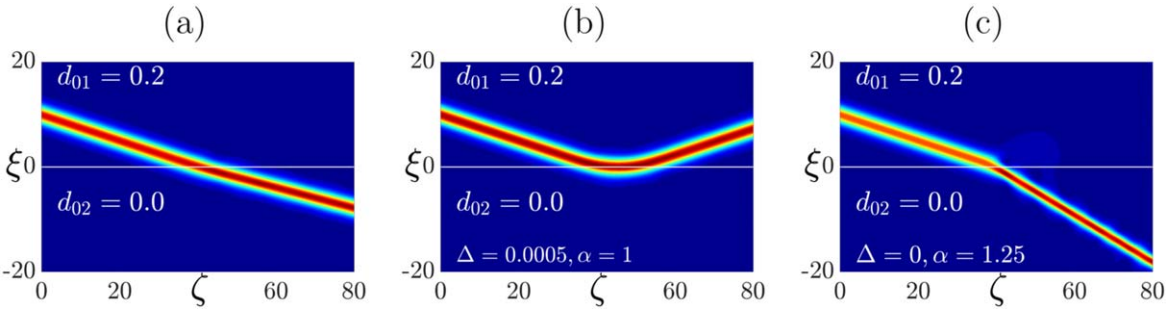

Figure 6. Soliton undergoing internal refraction at a diffusion step nonlocal interface (a). Total internal reflection (b) or external refraction (c) are achieved when $\Delta = 0.000\,5$ and $\alpha = 1.25$, respectively.

interface behavior under small changes of the local mismatch parameters. This analysis can be carried out by the definition of:

$$\delta = \Delta + 2\kappa\eta_0^2\left[\left(1 - \alpha\frac{\tau_2}{\tau_1}\right) + \frac{2}{3}\eta_0^2(\sigma_1 - \alpha\sigma_2)\right], \qquad (8)$$

which collects the contribution of a linear part Δ and an intensity-dependent term (through $2\kappa\eta_0^2$), which includes the Kerr and nonlocal mismatches. Equation (8) can easily address the type of refraction based solely on the sign of δ. External (internal) refraction is found when $\delta < 0$ ($\delta > 0$). Of course, $\delta = 0$ represents the absence of deflection, i.e. the total transparency condition.

The analysis of the system response to small changes of the interface parameters must first consider the limitations inherent to working within the framework of the Helmholtz theory [25, 26] where a weakly nonlocal regime [36, 48] is assumed. For example, when a fundamental soliton ($\eta_0 = 1$) with $\kappa = 2.5 \times 10^{-3}$ impinges a nonlocal diffusion step interface with $d_{01} = 0.2$ and $d_{02} = 0.0$, one obtains $\delta = 9 \times 10^{-5}$. Such a value of δ is responsible for the slight internal refraction that the soliton undergoes in figure 6(a).

We now alter the diffusion step nonlocal interface of figure 6(a) by changing significantly the local mismatches Δ and α, so that one works in a regime where the nonlocal contribution is completely masked by the local one. In figure 6(b), the condition $\Delta \gg 2\kappa\eta_0^2[(1 - \alpha\tau_2/\tau_1) + 2\eta_0^2/3(\sigma_1 - \alpha\sigma_2)]$ is satisfied and, instead of internal refraction, the linear mismatch is high enough to induce internal reflection. The scenario shown in figure 6(c) is, however, dominated by α, which not only leads to external refraction, but reduces significantly the soliton width. This regime would correspond to the one described in the upper right corner of table 1.

A different regime is found for $\Delta \sim 2\kappa\eta_0^2[(1 - \alpha\tau_2/\tau_1) + 2\eta_0^2/3(\sigma_1 - \alpha\sigma_2)]$, which is precisely the scenario addressed in [44] (see the bottom right corner of table 1). The role of diffusion here is limited to counteract the local mismatch by adding a quadratic dependence on soliton intensity, so that small variations on the intensity can alter the interface response. This can be seen in figure 7(a) that plots (8) as a function of soliton amplitude η_0 and where all interface parameters are properly chosen to induce, in this case, changes in the kind of refraction. The labels in figure 7(a) correspond to the soliton evolution in figures 7(b)–(d), respectively, where refraction (internal or external) is ruled by the sign of δ.

Nevertheless, the analysis of diffusion step nonlocal interfaces performed in this work can be carried out whenever local mismatches are much smaller than the nonlocal one. This condition, for the case of $\alpha = 1$, is found whenever $\Delta \ll 2\kappa\eta_0^2[(1 - \tau_2/\tau_1) + 2\eta_0^2/3(\sigma_1 - \sigma_2)]$, revealing that the smallness of Δ must always be considered in relation to the Helmholtz term $2\kappa\eta_0^2$. By assuming $\Delta = 0$ and $\alpha = 1$, we ensure that this condition is always met and the interface behavior is exclusively ruled by the diffusion of carriers.

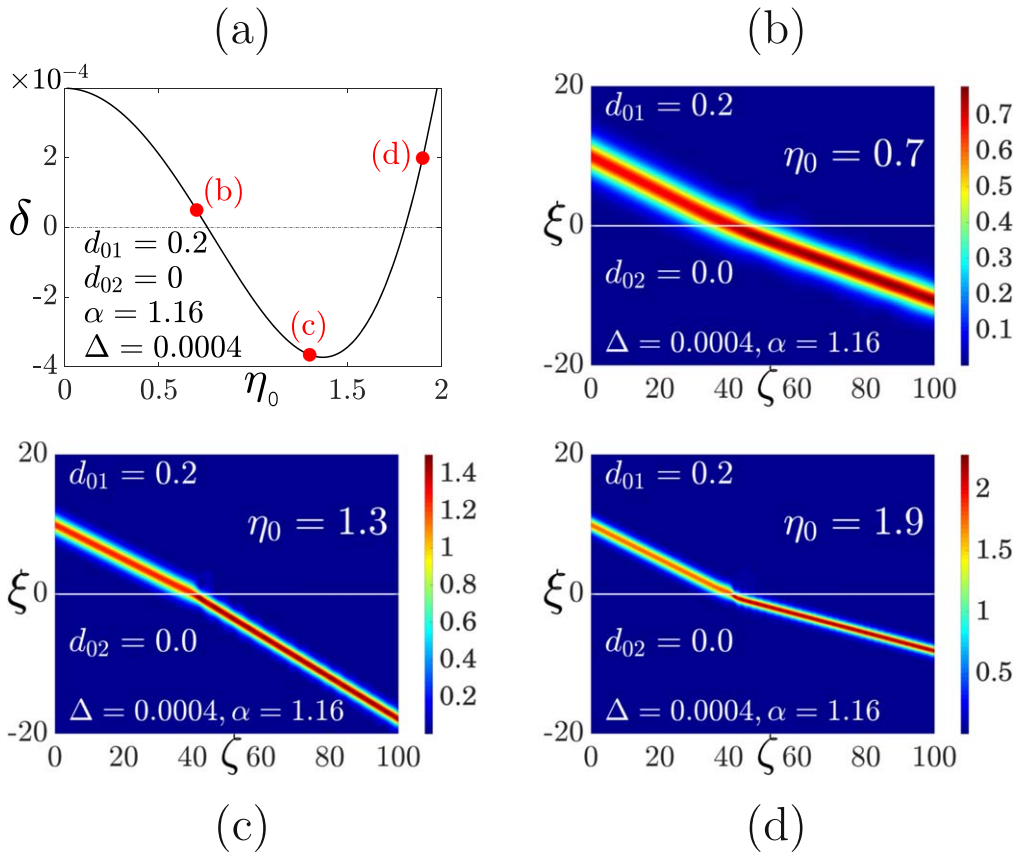

Figure 7. Equation (8) as a function of η_0 for a nonlocal interface. Soliton undergoing internal (b), external (c) and internal (d) refraction for different values of η_0.

5. Conclusions

This work has studied soliton evolution at diffusion step nonlocal interfaces within the framework of the Helmholtz theory. Following the guidelines of our previous works on interfaces, we have presented an analytical result that predicts how a soliton undergoes external (internal) refraction when the nonlocal response is higher (lower) in the second medium. With regards to total internal reflection, critical angles and giant GHSs have been found whenever the diffusion strength is higher in the first medium. The role of numerical simulations has been essential to contrast the validity of our model.

Acknowledgments

This work has been funded by the Spanish Ministerio de Economía y Competitividad (MINECO), project number TEC2015-69665-R (MINECO/FEDER, UE) and Junta de Castilla y León, project number VA296P18.

ORCID iDs

J Sánchez-Curto https://orcid.org/0000-0002-8160-7597

References

[1] Wright E M, Firth W J and Galbraith I 1985 Beam propagation in a medium with a diffusive Kerr-type nonlinearity *J. Opt. Soc. Am.* B **2** 383–6
[2] Andersen D R 1988 Surface-wave excitation at the interface between diffusive Kerr-like nonlinear and linear media *Phys. Rev.* A **37** 189–93
[3] Varatharajah P, Aceves A B, Moloney J V and Wright E M 1988 Stationary nonlinear surface waves and their stability in diffusive Kerr media *Opt. Lett.* **13** 690–2
[4] Varatharajah P, Newell A C, Moloney J V and Aceves A B 1990 Transmission, reflection and trapping of collimated light beams in diffusive Kerr-like nonlinear media *Phys. Rev.* A **42** 1767–74
[5] Aceves A B, Moloney J V and Newell A C 1989 Theory of light-beam propagation at nonlinear interfaces: I. Equivalent-particle theory for a single interface *Phys. Rev.* A **39** 1809–27
[6] Iturbe-Castillo M D, Sánchez-Mondragón J J and Stepanov S 1996 Formation of steady-state cylindrical thermal lenses in dark stripes *Opt. Lett.* **21** 1622–4
[7] Derrien F, Henninot J, Warenghem M and Abbate G 2000 A thermal (2d + 1) spatial optical soliton in a dye doped liquid crystal *J. Opt. A: Pure Appl. Opt.* **2** 332–7
[8] Kartasov Y V, Ye F, Vysloukh V A and Torner L 2007 Surface waves in defocusing thermal media *Opt. Lett.* **32** 2260–2
[9] Ye F, Kartasov Y V and Torner L 2008 Nonlocal surface dipoles and vortices *Phys. Rev. Lett.* **77** 033829
[10] Alfassi B, Rotschild C, Manela O, Segev M and Christodoulides D N 2007 Boundary force effects exerted on

solitons in highly nonlocal nonlinear media *Opt. Lett.* **32** 154–6
[11] Peccianti M and Assanto G 2012 *Phys. Rep.* **516** 147–208
[12] Peccianti M, Assanto G, Dyadyusha A and Kaczmarek M 2006 Tunable refraction and reflection of self-confined light beams *Nat. Phys.* **2** 737–42
[13] Peccianti M, Assanto G, Dyadyusha A and Kaczmarek M 2007 Nonspecular total internal reflection of spatial solitons at the interface between highly birefringent media *Phys. Rev. Lett.* **98** 113902
[14] Peccianti M, Assanto G, Dyadyusha A and Kaczmarek M 2007 Nonlinear shift of spatial solitons at a graded dielectric interface *Opt. Lett.* **32** 271–3
[15] Peccianti M and Assanto G 2007 Nematicons across interfaces: anomalous refraction and reflection of solitons in liquid crystals *Opt. Express* **15** 82599
[16] Piccardi A, Bortolozzo U, Residori S and Assanto G 2009 Spatial solitons in liquid-crystal light valves *Opt. Lett.* **34** 737–9
[17] Alberucci A, Piccardi A, Bortolozzo U, Residori S and Assanto G 2010 Nematicon all-optical control in liquid crystal light valves *Opt. Lett.* **35** 390–3
[18] Piccardi A, Alberucci A, Bortolozzo U, Residori S and Assanto G 2010 Readdressable interconnects with spatial soliton waveguides in liquid crystal light valves *IEEE Photonics Technol. Lett.* **22** 694–6
[19] Peccianti M, Conti C, Assanto G, De Luca A and Umeton C 2004 Routing of anisotropic spatial solitons and modulational instability in liquid crystals *Nature* **432** 733–7
[20] Conti C, Peccianti M and Assanto G 2005 Spatial solitons and modulational instability in the presence of large birefringence: the case of highly nonlocal liquid crystals *Phys. Rev.* E **72** 066614
[21] Alberucci A and Assanto G 2011 Nonparaxial (1 + 1)d spatial solitons in uniaxial media *Opt. Lett.* **36** 193–5
[22] Alberucci A and Assanto G 2011 Nonparaxial solitary waves in anisotropic dielectrics *Phys. Rev.* A **83** 033822
[23] Alberucci A, Jisha C P, Smyth N F and Assanto G 2015 Spatial optical solitons in highly nonlocal media *Phys. Rev.* A **91** 013841
[24] Fibich G 1996 Small beam nonparaxiality arrests self-focusing of optical beams *Phys. Rev. Lett.* **76** 4356–9
[25] Chamorro-Posada P, McDonald G S and New G H C 1998 Nonparaxial solitons *J. Mod. Optic.* **45** 1111–21
[26] Chamorro-Posada P, McDonald G S and New G H C 2000 Propagation properties of non-paraxial spatial solitons *J. Mod. Opt.* **47** 1877–86
[27] Akhmediev N, Ankiewicz A and Soto-Crespo J M 1993 Does the nonlinear Schrödinger equation correctly describe beam propagation? *Opt. Lett.* **18** 411–3
[28] Chamorro-Posada P, McDonald G S and New G H C 2002 Exact soliton solutions of the nonlinear Helmholtz equation *J. Opt. Soc. Am.* B **19** 1216–7
[29] Zakharov V E and Shabat A B 1972 Exact theory of two-dimensional self-focusing and one-dimensional self-modulation of waves in nonlinear media *Sov. Phys.—JETP* **34** 62–9
[30] Zakharov V E and Shabat A B 1973 Interaction between solitons in a stable medium *Sov. Phys.—JETP* **37** 823–8
[31] Chamorro-Posada P and McDonald G S 2003 Helmholtz dark solitons *Opt. Lett.* **28** 825–7
[32] Christian J M, McDonald G S and Chamorro-Posada P 2007 Bistable Helmholtz solitons in cubic-quintic materials *Phys. Rev.* A **76** 033833
[33] Christian J M, McDonald G S and Chamorro-Posada P 2010 Bistable dark solitons of a cubic-quintic Helmholtz equation *Phys. Rev.* A **81** 053831
[34] Christian J M, McDonald G S and Chamorro-Posada P 2007 Helmholtz solitons in power-law optical materials *Phys. Rev.* A **76** 033834
[35] Christian J M, McDonald G S and Chamorro-Posada P 2009 Bistable Helmholtz bright solitons in saturable materials *J. Opt. Soc. Am.* B **26** 2323
[36] Sánchez-Curto J and Chamorro-Posada P 2016 Helmholtz solitons in diffusive Kerr-type media *Phys. Rev.* A **93** 033826
[37] Chamorro-Posada P and McDonald G S 2006 Spatial Kerr soliton collision at arbitrary angles *Phys. Rev.* E **74** 036609
[38] Sánchez-Curto J, Chamorro-Posada P and McDonald G S 2007 Helmholtz solitons at nonlinear interfaces *Opt. Lett.* **32** 1126–8
[39] Sánchez-Curto J, Chamorro-Posada P and McDonald G S 2009 Nonlinear interfaces: intrinsically nonparaxial regimes and effects *J. Opt. A: Pure Appl. Opt.* **11** 054015
[40] Sánchez-Curto J, Chamorro-Posada P and McDonald G S 2011 Giant Goos-Hänchen shifts and radiation-induced trapping of Helmholtz solitons at nonlinear interfaces *Opt. Lett.* **36** 3605
[41] Sánchez-Curto J, Chamorro-Posada P and McDonald G S 2012 Helmholtz bright and black soliton splitting at nonlinear interfaces *Phys. Rev.* A **85** 013836
[42] Sánchez-Curto J, Chamorro-Posada P and McDonald G S 2010 Dark solitons at nonlinear interfaces *Opt. Lett.* **35** 1347–9
[43] Sánchez-Curto J, Chamorro-Posada P and McDonald G S 2011 Black and gray Helmholtz-Kerr soliton refraction *Phys. Rev.* A **83** 013828
[44] Sánchez-Curto J and Chamorro-Posada P 2017 Dual-switching behavior of nonlocal interfaces *Phys. Rev.* A **95** 053810
[45] Chamorro-Posada P and McDonald G S 2012 Time domain analysis of Helmholtz soliton propagation using the TLM method *J. Nonlinear Opt. Phys. Mater.* **21** 1250031
[46] Chamorro-Posada P, McDonald G S and New G H C 2001 Non-paraxial beam propagation methods *Opt. Commun.* **192** 1–12
[47] Chamorro-Posada P and McDonald G S 2014 Helmholtz non-paraxial beam propagation method: an assessment *J. Nonlinear Opt. Phys. Mater* **23** 1450040
[48] Krolikowski W and Bang O 2000 Solitons in nonlocal nonlinear media *Phys. Rev.* E **63** 016610
[49] Marcuse D 1980 Reflection of a Gaussian beam from a nonlinear interface *Appl. Opt.* **19** 3130–9
[50] Tomlinson W J, Gordon J P, Smith P W and Kaplan A E 1982 Reflection of a Gaussian beam at a nonlinear interface *Appl. Opt.* **21** 2041–51
[51] Emile O, Galstyan T, Le Floch A and Bretenaker F 1995 Measurement of the nonlinear Goos-Hänchen effect for Gaussian optical beams *Phys. Rev. Lett.* **75** 1511–3
[52] Shadrivov I V and Zharov A A 2002 Dynamics of optical spatial solitons near the interface between two quadratically nonlinear media *J. Opt. Soc. Am.* B **19** 596–602
[53] Chamorro-Posada P, Sánchez-Curto J, Aceves A B and McDonald G S 2014 Widely varying giant Goos-Hänchen shifts from airy beams at nonlinear interfaces *Opt. Lett.* **39** 1378–81
[54] Zhiwei S, Jing X, Jilong C, Yang L and Huagang L 2015 Goos-Hänchen shifts of Helmholtz solitons at nonlocal nonlinear interfaces *Eur. Phys. J.* D **69** 49
[55] Michinel H, Paz-Alonso M J and Pérez-García V M 2006 Turning light into a liquid via atomic coherence *Phys. Rev. Lett.* **96** 023903
[56] Smektala F, Quemard C, Couderc V and Barthélémy A 2000 Non-linear optical properties of chalcogenide glasses measured by z-scan *J. Non-Cyst. Solids* **274** 232

[57] Falcao-Filho E L, de Araújo C B, Boudebs G, Leblond H and Skarka V 2013 Robust two-dimensional spatial solitons in liquid carbon disulfide *Phys. Rev. Lett.* **110** 013901
[58] Cimek J, Liaros N, Couris S, Stepień R, Klimczak M and Buczyński R 2017 Experimental investigation of the nonlinear refractive index of various soft glasses dedicated for development of nonlinear photonic crystal fibers *Opt. Mater. Express* **7** 3471–83
[59] Dabby F W and Whinnery J R 1968 Thermal self-focusing of laser beams in lead glasses *Appl. Phys. Lett.* **13** 284–6
[60] Burzynski R, Singh B P, Prasad P N, Zanoni R and Stegeman G I 1988 Nonlinear optical processes in a polymer waveguide: grating coupler measurements of electronic and thermal nonlinearities *Appl. Phys. Lett.* **53** 2011–3
[61] Vicari L 2002 Pump-probe detection of optical nonlinearity in water-in-oil microemulsion *Philos. Mag.* B **82** 447–52